Inorg. Chem. **2009**, *48*, 267−276

On the Nature of the Reversibility of Hydration−Dehydration on the Crystal Structure and Magnetism of the Ferrimagnet $[Mn^{II}(enH)(H_2O)][Cr^{III}(CN)_6]\cdot H_2O$

Yusuke Yoshida,[†] Katsuya Inoue,*[,†] and Mohamedally Kurmoo*[,‡]

Department of Chemistry and Institute for Advanced Materials Research, Hiroshima University, Kagamiyama, Higashi-Hiroshima, 739-8526, Japan, and Laboratoire de Chimie de Coordination Organique, CNRS-UMR7140, Université Louis Pasteur, Institut Le Bel, 4 rue Blaise Pascal, 67000 Strasbourg Cedex 01, France

Received September 9, 2008

We report the synthesis, crystal structure, and thermal and magnetic properties of the two-dimensional achiral soft ferrimagnet $[Mn^{II}(enH)(H_2O)][Cr^{III}(CN)_6]\cdot H_2O$ (**1**), en = 1,2-diaminoethane, as well as the recyclability of the dehydration and rehydration and their influence on the crystal structure and its magnetic properties. Unlike [Mn(*S*-pnH)(H_2O)][Cr$(CN)_6$]$\cdot H_2O$ (**2*S***, pn = 1,2-diaminopropane), which is a chiral ($P2_12_12_1$) enantiopure ferrimagnet (T_C = 38 K), **1** crystallizes in the achiral orthorhombic *Pcmn* space group, having a similar two-dimensional square network of Mn−Cr with bridging cyanide, and **1** behaves also as a soft ferrimagnet (T_C = 42 K). X-ray diffraction experiments on a single crystal of **1** indicate a transformation from a single crystal to an amorphous phase upon dehydrataion and partial recovery of its crystallinity upon rehydration. The dehydrated phase **1-DP** exhibits long-range ordering at 75 K to a ferrimagnetic state and coercive field at 2 K of 100 Oe, which are a higher critical temperature and coercive field than for the virgin sample (H_C = 60 Oe). Thermogravimetric analyses indicate that the crystallinity deteriorates upon hydration−dehydration cycling, with persistence toward the amorphous phase, as also seen by magnetization measurements. This effect is associated with an increase of statistical disorder inherent in the dehydration−rehydration process. X-ray powder diffraction suggests that **1-DP** may retain order within the layers but loses coherence in the stacking of the layers.

Introduction

The considerable efforts that are being devoted in the development of magnetic materials based on molecules or molecular assemblies using organic linkers have resulted in a wide spectrum of metal−organic materials exhibiting long-range magnetic ordering at finite temperatures. In addition to the very wide range of Curie temperatures, based on ferromagnetism, ferrimagnetism, and canted-antiferromagnetism, improvement of several other parameters such as coercive field and remanent magnetization have been realized. Furthermore, the introduction of other properties such as optical or electrical properties has been successful, and responsive effects on the magnetism are being observed.[1−4] This growing interest in exploring multifunctional magnetic organic−inorganic hybrid materials is to address the existence of several properties within one material and to search for existing synergy with the aim of developing devices

* Authors to whom correspondence should be addressed. E-mail: kxi@hiroshima-u.ac.jp (K.I.); kurmoo@chimie.u-strasbg.fr (M.K.).
† Hiroshima University.
‡ Université Louis Pasteur.

(1) (a) Kurmoo, M.; Graham, A. W.; Day, P.; Coles, S. J.; Hursthouse, M. B.; Caulfield, J. L.; Singleton, J.; Pratt, F. L.; Hayes, W.; Ducasse, L.; Guioneeau, P. *J. Am. Chem. Soc.* **1995**, *117*, 12209. (b) Cororado, E.; Galán-Mascarós, J. R.; Gómez-García, C. J.; Laukhin, V. *Nature* **2000**, *408*, 447. (c) Uji, S.; Shinagawa, H.; Terashima, T.; Yakabe, T.; Terai, Y.; Tokumoto, M.; Kobayashi, A.; Tanaka, H.; Kobayashi, H. *Nature* **2001**, *410*, 908. (d) Cororado, E.; Day, P. *Chem. Rev.* **2004**, *104*, 5419. (e) Kobayashi, H.; Cui, H.-B.; Kobayashi, A. *Chem. Rev.* **2004**, *104*, 5265. (f) Ohkoshi, S.; Tokoro, H.; Matsuda, T.; Takahashi, H.; Irie, H.; Hashimoto, K. *Angew. Chem., Int. Ed.* **2007**, *46*, 3238. (g) Gu, Z.-G.; Zhou, X.-H.; Jin, Y.-B.; Xiong, R.-G.; Zuo, J.-L.; You, X.-Z. *Inorg. Chem.* **2007**, *46*, 5462. (h) Cui, H. B.; Wang, Z.; Takahashi, K.; Okano, Y.; Kobayashi, H.; Kobayashi, A. *J. Am. Chem. Soc.* **2006**, *128*, 15074.
(2) Ti, T.; Tancrez, N; Clement, R.; Ledoux-Rax, I.; Zyss, J. *J. Lumin.* **2004**, *110* (4), 389.
(3) Murayama, A.; Sakuma, M. *Appl. Phys. Lett.* **2006**, *88*, 122504.

10.1021/ic801734x CCC: $40.75
Published on Web 12/01/2008

suitable for particular applications. These combinations now include magnetism and conductivity, ferro or antiferroelectricity, nonlinear-optical activity, porosity with guest dependence,[5−9] or chirality.[10−14] In the past few years, we have been searching for chiral magnets, in particular, to look for new physical phenomena as well as to understand the relationship between structural chirality and magnetic chirality and how they can be coupled. Although there has been much theoretical work done predicting interesting phenomena, experimental evidence of these is still lacking due to the lack of suitable materials. One such experiment concerns the observation of the magneto-chiral dichroism for a chiral paramagnet and is yet to be explored for a magnetically ordered chiral materials.[15] A recent theoretical study on the effect of the presence of chirality on the magnetic properties points to the coupling of the orbital and the spin momenta via a Dzyaloshinski−Moriya interaction similar to that for weak ferromagnetism.[16]

In this context, chirality with magnetism is of special interest. One chiral magnet among the few which are known was reported by Inoue et al. by employing a simple chiral diamine, *S*-1,2-diaminopropane, to produce the ferrimagnet $[Mn^{II}(S\text{-pnH})(H_2O)][Cr^{III}(CN)_6]\cdot H_2O$ (**2*S***).[11] This compound crystallizes in the chiral orthorhombic space group $P2_12_12_1$, and it has a two-dimensional network structure. Below the Curie temperature ($T_C = 38$ K), the saturation magnetization is $2\mu_B$, due to antiferromagnetic ordering of Cr^{3+} ($S = 3/2$) and Mn^{2+} ($S = 5/2$). So far, μ-SR, powder neutron diffraction, single-crystal neutron diffraction, and extensive nonlinear magnetization measurements have been performed, and these suggest that the magnetism is inherently coupled to the chirality,[17] for example, an enhanced third-order ac susceptibility which is strongly dependent on the applied field and oscillation frequency.[17d] To test these hypotheses, we have explored the use of ethylenediamine or racemic 1,2-diaminopropane in the place of enantiopure 1,2-diaminopropane to produce achiral systems for comparison. The present paper deals with further experiments concerning the recyclability of the crystal structure and its consequence on the magnetism of an achiral congener, $[Mn^{II}(enH)(H_2O)][Cr^{III}(CN)_6]\cdot H_2O$ (**1**). In a preliminary study, we observed a transformation from single-crystallinity to an amorphous phase upon dehydration and its return to a crystalline phase upon rehydration. These transformations are associated with considerable changes in the magnetic properties.[6a] Here, we report further study using thermogravimetry, to understand the recyclability of the dehydration−rehydration and the associated changes in the structural and magnetic properties of **1**.

Experimental Section

Synthesis of Starting Materials, $K_3[Cr(CN)_6]$ and en·2HCl. $K_3[Cr(CN)_6]$ was synthesized by a slight modification to the reported procedure.[18] For en·2HCl, a solution of 10 mL of ethylenediamine ($d = 0.899$ g/mL, 150 mmol) in 30 mL of H_2O was added to 30 mL of 37% HCl ($d = 1.19$ g/mL, 362 mmol). The mixture was evaporated to yield a white powder, which was then dissolved in a minimum amount of hot water. The concentrated hot solution was cooled down to room temperature, and EtOH was added while stirring until no more white precipitation occured. The precipitate was filtered and washed with EtOH and ether. Yield: 19.1 g, 96%.

Synthesis of $[Mn(enH)(H_2O)][Cr(CN)_6]\cdot H_2O$ (1). This compound was prepared as reported in the literature.[6a] Anal. calcd for

(4) (a) Ohkoshi, S.; Ikeda, S.; Hozumi, T.; Kashiwagi, T.; Hashimoto, K. *J. Am. Chem. Soc.* **2006**, *128*, 5320. (b) Li, D.; Clérac, R.; Roubeau, O.; Harté, E.; Mathonière, C.; Bris, R. L.; Holmes, S. M. *J. Am. Chem. Soc.* **2008**, *130*, 252. (c) Bonhommeau, S.; Molnár, G.; Galet, A.; Zwick, A.; Real, J.-A.; McGarvey, J. J.; Bousseksou, A. *Angew. Chem., Int. Ed.* **2005**, *44*, 4069. (d) Hayami, S.; Motokawa, N.; Shuto, S.; Masuhara, N.; Someya, T.; Ogawa, Y.; Inoue, K.; Maeda, Y. *Inorg. Chem.* **2007**, *46*, 1789. (e) Herrera, J. M.; Marvaud, V.; Verdaguer, M.; Marrot, J.; Kalisz, M.; Mathoniére, C. *Angew. Chem., Int. Ed.* **2004**, *43*, 5468. (f) Sato, O. *Acc. Chem. Res.* **2003**, *36*, 692. (g) Sato, O.; Iyoda, T.; Fujishima, A.; Hashimoto, K. *Science* **1996**, *272*, 704.

(5) Kaneko, W.; Ohba, M.; Kitagawa, S. *J. Am. Chem. Soc.* **2007**, *129*, 13706.

(6) (a) Yoshida, Y.; Inoue, K.; Kurmoo, M. *Chem. Lett.* **2007**, *37*, 504. (b) Yoshida, Y.; Inoue, K.; Kurmoo, M. *Chem. Lett.* **2007**, *37*, 586.

(7) Niel, V.; Thompson, A. L.; Munoz, M. C.; Galet, A.; Goeta, A. E.; Real, J. A. *Angew. Chem., Int. Ed.* **2003**, *42*, 3759.

(8) (a) Yanai, N.; Kaneko, W.; Yoneda, K.; Ohba, M.; Kitagawa, S. *J. Am. Chem. Soc.* **2007**, *129*, 3496. (b) Maspoch, D.; Ruiz-Molina, D.; Wurst, K.; Domingo, N.; Gavallini, M.; Biscarini, F.; Tajada, J.; Rovira, C.; Veciana, J. *Nat. Mater.* **2003**, *2*, 190.

(9) (a) Ohkoshi, S.; Tsunobuchi, Y.; Takahashi, H.; Hozumi, T.; Shiro, M.; Hashimoto, K. *J. Am. Chem. Soc.* **2007**, *129*, 3084. (b) Nihei, M.; Han, L.; Oshio, H. *J. Am. Chem. Soc.* **2007**, *129*, 5312. (c) Kurmoo, M.; Kumagai, H.; Akita-Tanaka, M.; Inoue, K.; Takagi, S. *Inorg. Chem.* **2006**, *45*, 1627. (d) Galet, A.; Muñoz, M. C.; Real, J. A. *Chem. Commun.* **2006**, 4321. (e) Zeng, M.-H.; Feng, Z.-L.; Zhang, W.-X.; Chen, Z.-M. *Dalton Trans.* **2006**, 5294. (f) Kurmoo, M.; Kumagai, H.; Chapman, K. W.; Kepert, C. J. *Chem. Commun.* **2005**, 3012. (g) Ohkoshi, S.; Arai, K.; Sato, Y.; Hashimoto, K. *Nature Mat.* **2004**, *3*, 857. (h) Wang, Z.; Zhang, B.; Fujiwara, H.; Kobayashi, H.; Kurmoo, M. *Chem. Commun.* **2004**, 416. (i) Halder, G. J.; Kepert, C. J.; Moubaraki, B.; Murray, K. S.; Cashion, J. D. *Science* **2002**, *298*, 1762.

(10) (a) Kaneko, W.; Ohba, M.; Kitagawa, S. *J. Am. Chem. Soc.* **2007**, *129*, 248. (b) Milon, J.; Daniel, M.-C.; Kaiba, A.; Guionneau, P.; Brandès, S.; Sutter, J.-P. *J. Am. Chem. Soc.* **2007**, *129*, 13872. (c) Higashikawa, H.; Okuda, K.; Kishine, J.; Masuhara, N.; Inoue, K. *Chem. Lett.* **2007**, *36*, 1022. (d) Imai, H.; Inoue, K.; Kikuchi, K.; Yoshida, Y.; Ito, M.; Sunahara, T.; Onaka, S. *Angew. Chem., Int. Ed.* **2004**, *43*, 5618. (e) Coronado, E.; Gómez-García, C. J.; Nuez, A.; Romeo, F. M.; Rusanov, E.; Stoeckli-Evans, H. *Inorg. Chem.* **2002**, *41*, 4615. (f) Inoue, K.; Imai, H.; Ghalsasi, P. S.; Kikuchi, K.; Ohba, M.; Okawa, H.; Yakhmi, J. V. *Angew. Chem., Int. Ed.* **2001**, *40*, 4242.

(11) Inoue, K.; Kikuchi, K.; Ohba, M.; Okawa, H. *Angew. Chem., Int. Ed.* **2003**, *42*, 4810.

(12) (a) Akita-Tanaka, M.; Kumagai, H.; Markosyan, A.; Inoue, K. *Bull. Chem. Soc. Jpn.* **2007**, *80*, 204. (b) Numata, Y.; Inoue, K.; Baranov, N.; Kurmoo, M.; Kikuchi, K. *J. Am. Chem. Soc.* **2007**, *129*, 9902. (c) Munguet, M.; Luneau, D.; Lhotel, E.; Villar, V.; Paulsen, C.; Amabilino, D. B.; Veciana, J. *Angew. Chem., Int. Ed.* **2002**, *41*, 586. (d) Kumagai, H.; Inoue, K. *Angew. Chem., Int. Ed.* **1999**, *38*, 1601.

(13) (a) Coronado, E.; Galán-Mascarós, J. R.; Gómez-García, C. J.; Mursia-Martínez, A. *Chem.—Eur. J.* **2006**, *12*, 3484. (b) Zeng, M.-H.; Wang, B.; Wang, X.-Y.; Zhang, W.-X.; Chen, X.-M.; Gao, S. *Inorg. Chem.* **2006**, *45*, 7069.

(14) Zhang, B.; Wang, Z.; Kurmoo, M.; Gao, S.; Inoue, K.; Kobayashi, H. *Adv. Funct. Mater.* **2007**, *17*, 577.

(15) Rikken, G. L. J. A.; Raupach, E. *Nature.* **1997**, *390*, 493.

(16) (a) Dzyaloshinski, I. *J. Phys. Chem. Solids* **1958**, *4*, 241. (b) Moriya, T. *Phys. Rev.* **1960**, *120*, 91.

(17) (a) Kishine, J.; Inoue, K.; Yoshida, Y. *Prog. Theor. Phys. Suppl.* **2005**, 82. (b) Hoshikawa, A.; Kamiyama, T.; Purwanto, A.; Ohishi, K.; Higemoto, W.; Ishigaki, T.; Imai, H.; Inoue, K. *J. Phys. Soc. Jpn.* **2004**, *73*, 2597. (c) Ohishi, K.; Higemoto, W.; Koda, A.; Saha, S. R.; Kadono, R.; Inoue, K.; Imai, H.; Higasikawa, H. *J. Phys. Soc. Jpn.* **2006**, *75*, 063705. (d) Inoue, K.; Kishine, J.; Mito, M.; Kikuchi, K.; Imai, H.; Yoshida, Y.; Ohsumi, H. Manuscript in preparation.

(18) (a) Uehara, A.; Kaizaki, S. *Jikken kagaku kouza 17: Muki sakutai · Kire-to sakutai* (in Japanese), 4th ed.; Nihon kagaku kai Ed.: Tokyo, 1991; p 60. (b) Schaap, B. W.; Krishnamurthy, R.; Wakefield, D. K.; Coleman, W. F. *Coordination Chemistry*; Kirschner, S., Ed.; Plenum: New York, 1969; p 177.

1, $C_8H_{13}CrMnN_8O_2$ (%): C, 26.52; H, 4.17; N, 30.98. Found: C, 26.57; H, 3.98; N, 31.01.

Single-Crystal X-Ray Diffraction. All of the diffraction data were collected using a Bruker SMART-APEX diffractometer equipped with a CCD area detector and graphite-monochromated Mo Kα radiation ($\lambda = 0.71073$ Å) at the Natural Science Center for Basic Research and Development (N-BARD), Hiroshima University. Single crystals of **1** and **2*S*** were separately glued to glass fibers using Araldite, and intensity data were collected by in situ measurement through the ω-scan mode (0.3° steps). Semiempirical absorption corrections on Laue equivalents were applied. The structures were solved by direct methods and refined by full-matrix least squares against F^2 for all data using SHELX-97. For virgin **1** and rehydrated **1-HP**, hydrogen atoms bonded to carbon atoms were included in calculated positions. The positions of the hydrogen atoms on O(1) were located from the difference Fourier map. The positions of the hydrogen atoms on the oxygen atom were located from the different Fourier map unless the refinement was unstable. In all cases, non-hydrogen atoms were refined anisotropically.

Elemental Analyses. Elemental analyses for C, H, and N were performed on a Perkin-Elmer 2400II at the Natural Science Center for Basic Research and Development (N-BARD), Hiroshima University.

Infrared Spectroscopy. Infrared spectra were recorded by transmission through KBr disks containing ca. 0.5% of the compounds using a HORIBA FT-IR spectrometer FT-720. For **1-DP**, some powdered KBr containing the virgin sample was vacuumed at 383 K for 2 h and then pressed into a disk. For **1-HP**, a virgin sample of **1** was heated to 363 K and cooled down to room temperature under a nitrogen atmosphere; then, the dehydrated sample was soaked into distilled water and dried in the nitrogen atmosphere. The rehydrated sample was mixed with KBr and pressed into a disk.

Magnetic Measurements. Magnetic measurements were carried out by use of a Quantum Design MPMS-5S SQUID magnetometer. Diamagnetic corrections were estimated using Pascal constants (-1.783×10^{-4}, -1.523×10^{-4}, and -1.765×10^{-4} cm^3 mol^{-1} respectively for virgin **1**, dehydrated **1-DP**, and rehydrated **1-HP**, which is assumed to show 93% rehydration, as can be seen in the thermogravimetric (TG) results)[19] and background correction by experimental measurement of an empty gelatin capsule.

The data were collected for virgin **1**, followed by those for the dehydrated **1-DP**, and finally for rehydrated **1-HP**. The dehydrated **1-DP** was obtained in situ by heating the virgin sample in a flow of helium from 310 to 360 K at a warming rate of 0.5 K/minute in the SQUID magnetometer. For the hydrated phase, several runs were performed at different exposure times to humid air and, finally, for a sample soaked in distilled water to obtain **1-HP**. The phase state was verified by locating the magnetic critical temperature after each transformation.

Temperature dependence of the magnetic susceptibilities for all phases was performed in an applied field of 100 Oe. For the dehydrated samples **1-DP**, magnetic susceptibilities were collected upon cooling from 360 to 2 K. For the other phases, magnetic susceptibilities were collected upon cooling from 300 to 2 K. Isothermal magnetization at 2 K was measured for each phase from −50 to +50 kOe.

For further investigation of the temperature dependence of magnetization in a low field, a new sample was placed into the SQUID magnetometer, and zero-field-cooled (ZFC) measurement and field-cooled (FC) measurement were carried out in a measuring field of 5 Oe for virgin **1**, dehydrated **1-DP**, and rehydrated **1-HP** using the same protocol for transforming between the phases described earlier.

Thermogravimetric Analyses. TG measurements were performed on several samples of **1** (on 10.574 mg for the data reported here) using a Rigaku Instrument TG8120 operating under dry nitrogen with heating from room temperature (ca. 290 K) to 363 K at a rate of 1 K/min, and cooling down to room temperature at a rate of 10 K/min. After cooling, the sample was placed overnight in a closed plastic box containing water kept at ≈ 310 K. The rehydrated sample was placed into the machine, and the same measurement was repeated four consecutive times. Further measurements were performed to higher temperatures by use of a Perkin-Elmer Pyris 6 TGA operating under dry nitrogen at a heating rate of 5 K/min for 18.343 mg of **1**.

Powder X-Ray Diffraction. The powder X-ray diffraction (PXRD) patterns were measured on a Rigaku Rint 2000 system using Cu Kα radiation and employing a scan rate of 4.0°/min and a step of 0.02°. The sample was transformed from virgin **1** to dehydrated **1-DP**, and then to rehydrated **1-HP**. Dehydrated **1-DP** was obtained by placing the sample in a heated desiccator kept at 360 K for 10 min under nitrogen. Hydrated **1-HP** was obtained by exposing the dehydrated sample to air for 1 h. The simulated patterns were calculated from the single-crystal X-ray data using RIETAN-2000.[20]

Preparation of Hydrated Sample for Physical Measurements. Different methods are employed for hydration of the sample. For single-crystal X-ray and PXRD measurement, the Bragg diffraction peaks were easily recovered by exposing the sample to air for ca. 1 h. For SQUID measurements, the sample is contained within a gelatin capsule, and this slows the rehydration by water from air. Therefore, a drop of water was added to the dehydrated sample and allowed to dry, and magnetization was measured again. This method is also used for IR measurement. For TG measurements, the uptake of water from air takes a long time due to the presence of only one small hole in the sample compartment. Consequently, a drop of water was added to the dehydrated sample, but there was difficulty putting all iterative measured data onto the same scale. Finally, the TG results were obtained by placing the dehydrated sample under high-humidity conditions overnight.

Results and Discussion

Thermogravimetric Analyses. The TG measurements were performed on several samples consisting of powdered crystals of **1** under a nitrogen atmosphere. In each case, the sample shows a first weight loss starting at 340 K and attains a plateau at 360 K, which is stable up to 480 K, where it decomposes (Figure 1). The observed percentage weight loss (9.8%) is close to the value for the departure of two water molecules per formula unit (10.0%). Upon lowering the temperature of the samples having been heated only to 363 K under nitrogen, the sample weight is slightly increased. Upon exposure of the samples to high-humidity air (humidity ≈ 93%, temperature ≈ 310 K) overnight, they reabsorb water and recover 93% of the water molecules. This recovery process was labeled as dehydrated **1-DP** to rehydrated **1-HP**. Dehydration−rehydration processes are not perfectly reversible, and the iterative measurement showed a slightly lower

(19) Kahn, O. *Molecular Magnetism*; Wiley-VCH: New York, 1993; p 3.

(20) Izumi, F.; Ikeda, T. *Mater. Sci. Forum* **2000**, *321−324*, 198.

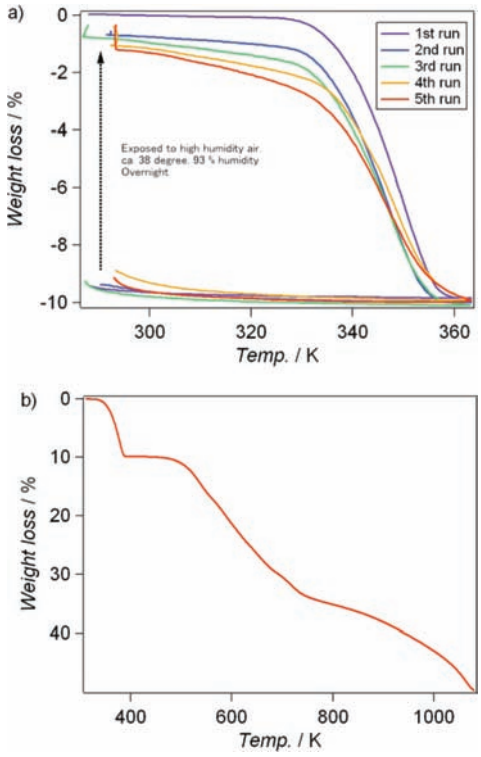

Figure 1. (a) Thermogravimetric curve for low-temperature region and (b) high-temperature region for **1**.

and lower rehydration ratio (92%, 90%, 88%, and 88%, for after second, third, fourth, and fifth runs), describing the formation of irreversible domains through every cycle. Except for the virgin sample in the first run, a sudden drop of the weight at the start of the subsequent measurements can be seen, indicating that there are water molecules on the surface that are easily removed when the sample is placed under a nitrogen atmosphere. In our previous communication,[6] we had mistakenly claimed that **1** recovers its initial weight when it was exposed to air in the absence of iterative measurements.

An independent measurement under nitrogen to 1100 K shows an additional gradual weight loss from 470 K to a metastable compound at 750 K, which has a mass corresponding to $MnCr(CN)_5$ and is followed by another continuous weight loss to 1100 K (Figure 1b).

Infrared Spectroscopy. The infrared spectra of the virgin (**1**), dehydrated (**1-DP**), and rehydrated phases (**1-HP**) are shown in Figure 2. The bands can be assigned using group frequencies as follows (Table 1). The asymmetric and symmetric stretching modes of the water molecules are observed at the highest energy at 3600 and 3523 cm^{-1}, respectively. These two bands are absent from the spectrum of **1-DP**, confirming the complete dehydration of **1**, and they are observed again in the spectrum of **1-HP**, showing the rehydration. The corresponding N−H stretching modes and those of C−H are observed at lower energies. We note that sharpening of some of these bands is observed in the spectrum of **1-DP** compared to those of **1** and **1-HP**, which may be related to the presence of hydrogen bonds. Three sharp bands of stretching modes of the cyanide are observed in the spectra of **1** and **1-HP**, where the intensities are

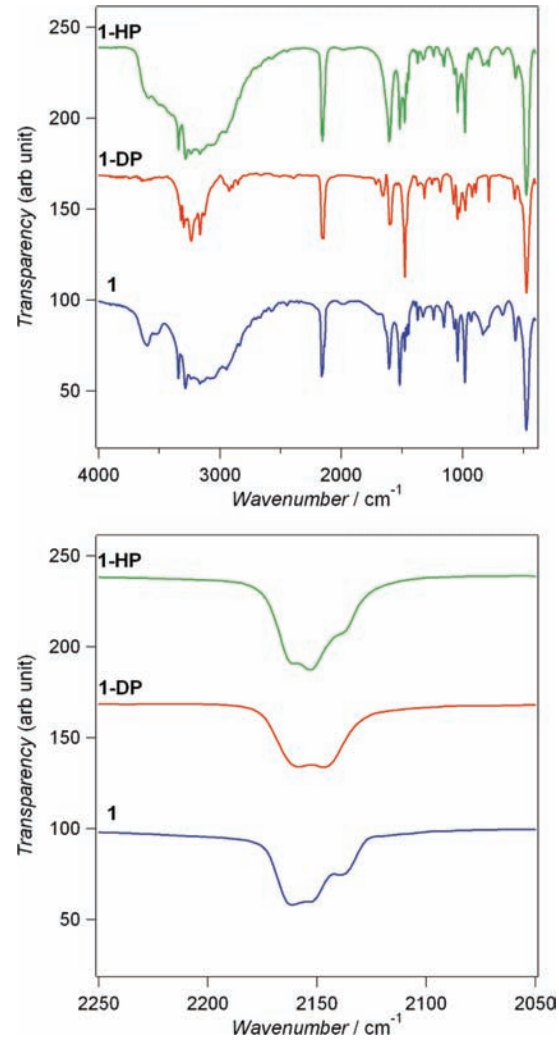

Figure 2. Infrared transmission spectra of **1**, dehydrated **1-DP**, and rehydrated **1-HP**.

approximately 2:2:1, which may suggest that the weaker one is associated with the noncoordinating cyanide. However, for **1-DP**, there are only two peaks of equal intensities, which suggests slight asymmetry or nonequivalence between the six bridging cyanides. Other modes of the ethylenediamine ligand are observed between 700 and 1700 cm^{-1}. A very strong peak at 474 cm^{-1} seen in all spectra may be due to the Cr−C mode.

Crystal Structure. In the first magnetization experiment of this compound, we realize a large increase of the Curie temperature upon in situ dehydration in a SQUID and its partial reversibility upon rehydration in the air (see magnetization results later). Consequently, we examine the X-ray diffraction of a single crystal by performing data collections while cycling the temperature. Some of the observations were similar to those made by Ohba et al., who reported the structures and magnetism of $[Mn(NNdmenH)(H_2O)][Cr(CN)_6]\cdot H_2O$ (**3**; NNdmen = *N*,*N*-dimethylethylenediamine)[5] and also to those of $[Mn(rac\text{-pn})(H_2O)][Cr(CN)_6]\cdot H_2O$ (***2rac***; pn = 1,2-diaminopropane).[6b] The latter two studies have shown that single-crystal to single-crystal transformations upon

Table 1. Frequencies and Assignments of the Bands in the Spectra of the **1**, **1-DP**, and **1-HP**

1	1-DP	1-HP		1	1-DP	1-HP	
3600 m		3590 m	ν(O−H)		1593 s		δ(N−H)
3523 m		3502 m	ν(O−H)	1519 s		1520 s	δ(C−H)
3342 s		3340 s	ν(N−H)	1477 m	1475 vs	1477 s	δ(C−H)
	3323 m	3322 s	ν(N−H)	1462 m		1460 m	δ(C−H)
3284 s	3298 s	3284 s	ν(N−H)	1446 m		1448 m	δ(C−H)
3236 s	3238 s	3240 s	ν(N−H)	1371 w	1369 w	1371 w	
3164 s	3165 s	3166 s	ν(N−H)	1329 w	1315 m	1327 w	
	3130 m	3132 s	ν(N−H)	1240 w	1254 w	1240 w	
3066 s		3056 s		1184 m	1184 m	1182 w	ν(C−N)
2966 s		2964 s	ν(C−H)			1153 w	ν(C−N)
2947 s	2924 m	2947 s	ν(C−H)	1103 vw	1074 m	1103 w	ν(C−N)
2839 m	2897 w	2841 m	ν(C−H)	1068 m	1043 m	1066 m	ν(C−N)
	2852 w		ν(C−H)	1041 s	1026 m	1041 m	ν(C−N)
	2831 vw		ν(C−H)	982 s	980 m	981 s	ν(C−N)
2162 s	2158 s	2161 s	ν(C−N)	931 w	922 m	930 w	δ(N−H)
2152 s	2146 s	2154 s	ν(C−N)		891 m		δ(N−H)
2139 m		2139 m	ν(C−N)	833 m		833 w	δ(N−H)
1990 vw				785 m	785 m	784 w	δ(N−H)
	1714 w			669 w		669 w	
	1658 m			565 w	570 m	565 m	
1606 s	1600 s	1606 s	δ(N−H)	476 vs	474 vs	476 vs	ν(Cr−C)

dehydration are accompanied by a change from 2D to 3D through cyanide bridges between Cr and Mn and an increase in the Curie temperatures.

To explore this particular observation further, we performed in situ experiments by determining first the crystal structure of a virgin crystal of **1**, then of **1-DP**, and finally of **1-HP**. As can be seen in Figure 3, when the crystal was heated to 360 K, the diffraction spots smeared out and disappeared (see movie 1 in the Supporting Information), indicating dehydration results in an amorphous phase. However, when the crystal was exposed to air, the diffraction spots were recovered (see movie 2 in the Supporting Information) to realize the same crystal structure as the virgin sample.

Crystal Structure of Virgin 1 and Its Rehydrated Form 1-HP. Details of the crystal data are given in Table 2, and a list of the bond distances and angles is given in Table 3. X-ray structural analyses of the diffraction data on a single crystal of **1** suggest an achiral orthorhombic *Pcmn* space group, compared to a chiral orthorhombic $P2_12_12_1$ for **2*S***, containing the optically pure *S*-1,2-diaminopropane (see the Supporting Information),[11] achiral monoclinic $P2_1/m$ for **2*rac***, containing racemic 1,2-diaminopropane,[6b] and $P2_1/c$ for **3**, containing *N*,*N*-dimethylethylenediamine.[5] The space group *Pcmn* has a mirror plane perpendicular to the *b* axis, an *n* glide symmetry, and an inversion center, as a consequence of using achiral amine and ethylenediamine, which is disordered on two positions. The Mn and the two nitrogen atoms of ethylenediamine are on the mirror plane, and the Cr atom is located on an inversion center. The common key feature of all of the crystal structures is the 2D-square grid of Mn and $Cr(CN)_4$, where the Mn and Cr alternate in the *ab* plane and are bridged by cyanide (Figure 4). However, the layers are not planar but are corrugated where the corrugation propagates along the *b* axis, and they are in phase with the neighboring layers. Viewing along the *c* axis, that is, perpendicular to the layers, we find that adjacent layers are staggered. In the two-dimensional sheet, the average separation between the Mn and Cr atoms through the cyanide bridge is 5.3308(7) Å for **1**, which is slightly shorter than that for **2*S*** (5.3490(14) Å).[21] The shortest intersheet metal−metal separation for **1** is observed between the Mn and Cr atoms (7.4984(7) Å), while the intersheet homometallic contacts are longer than 8.3066(9) Å. From the viewpoint of the magnetic dipole interaction, a distance of less than 10 Å describes a ferromagnetic interaction between the two-dimensional sheets, which is the same situation as for **2*S***.

Coming out of the two-dimensional sheets, two more cyanide groups complete the octahedral coordination of the chromium while the amine and one water molecule are coordinated trans to each other in the axial positions of the manganese. Compounds **1**, **2*S***, **2*rac***, and **3** differ by the presence of different amines which occupy the interlayer gallery (Figure 4). As can be seen in Table 3, Mn(1)−N/O distances range from 2.198(2) to 2.303(3) Å, and N−Mn−N/O angles are in the range of 85.04(7)−94.01(8)° and 176.87(11)−178.74(8)° for cis and trans positions. The Cr(1)−C distances range from 2.062(3) to 2.066(2) Å, and C−Cr−C angles are in the range of 88.36(10)−91.64(10)° for cis positions. These values suggest small distortion from perfect octahedral geometries for the two transition metals.

Between the two-dimensional sheets, the nitrogen atom N(5) of the noncoordinating amine forms two hydrogen bonds with the oxygen atoms of the crystal water molecules, (N(5)···O(2), 2.831(9) Å), and with the oxygen atom of coordinating water (N(5)···O(1′), 2.937(4) Å). Furthermore, the oxygen atom O(1) of the coordinating water is found to have two hydrogen bonds with the nitrogen of the cyanide group in neighboring layer (O(1)···N(3′), 2.752(4) Å). One hydrogen bond is generated by mirror symmetry from the other.

(21) To compare the crystal structures of the Mn−Cr Prussian blue analogues (**1**, **2*rac***, and **2*S***), **2*S*** was synthesized, and single-crystal X-ray measurements at room temperature using the same experimental conditions as for **1** and **2*rac*** were performed (see Supporting Information).

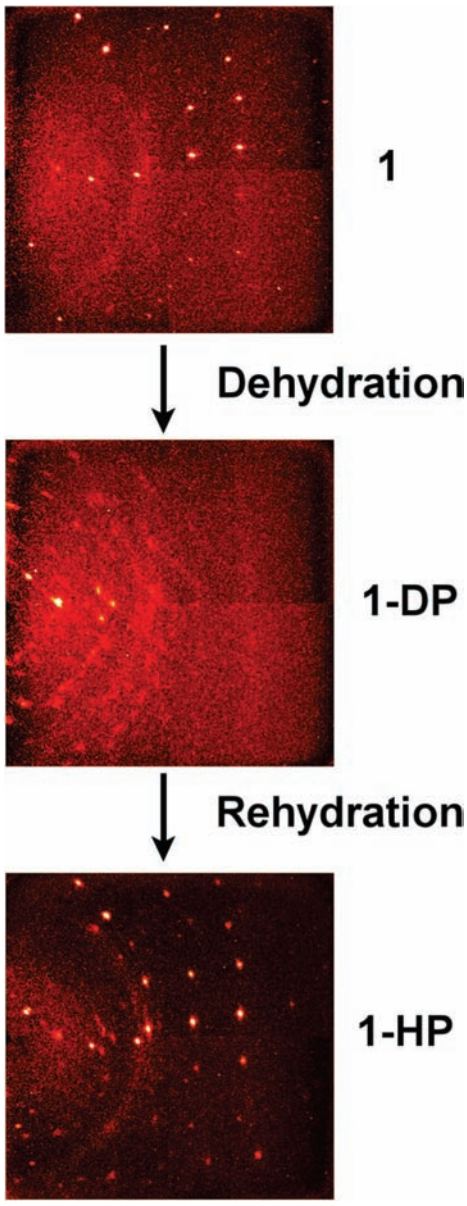

Figure 3. Observed Bragg diffraction spots of a single crystal before (top, 295 K) and after dehydration (middle, 360 K; it remains the same after rapid cooling to 295 K) and upon exposure to the air for 12 min (bottom, 295 K).

Crystal Structure of the Dehydrated Phase 1-DP. Attempts to collect diffraction data for the dehydrated crystal under different conditions failed as practically all of the Bragg diffractions disappeared upon dehydration. However, magnetic measurement showed an increase of about 30 K in the Curie temperature (see below), suggesting the formation of a 3-D structure, as demonstrated for ***2rac*** and **3**.[5,6] The dehydration of the latter compounds changes the crystal system from having a 2D magnetic dimensionality to a 3D one and is accompanied by an increase of the Curie temperature from 36 to 70 K for ***2rac*** and from 35.2 to 60 K for **3**.

Interestingly, the Bragg diffractions are recovered with almost the same quality after exposure of the same crystal to air. In the crystal structure of **1**, ethylenediamine coordinates to the Mn atom in two ways (statistically at random),

Table 2. Crystallographic Data for Virgin **1** and Rehydrated **1-HP**

Compound	virgin **1**	rehydrated **1-HP**[a]
formula	$C_8H_{13}CrMnN_8O_2$	$C_8H_{13}CrMnN_8O_2$
fw	360.20	360.20
T, K	298	298
atmosphere	air	air
exposure time, s	10	20
no. of frames	830	830
cryst syst	orthorhombic	orthorhombic
space group	*Pcmn*[b]	*Pcmn*[b]
a, Å	7.5177(8)	7.5298(9)
b, Å	14.6493(15)	14.6804(19)
c, Å	14.9539(15)	14.9760(19)
V, Å^3	1646.9(3)	1655.5(4)
Z	4	4
D_C, g/cm^3	1.453	1.445
μ (Mo Kα), mm^{-1}	1.438	1.431
cryst size, mm^3	0.6 × 0.2 × 0.1	0.6 × 0.2 × 0.1
T_{min}, T_{max}	0.5316, 1.0000	0.7784, 1.0000
θ_{min}, θ_{max} (deg)	2.710, 27.839	3.028, 27.96
total no. reflns	6353	6009
no. unique reflns (R_{int})	1950	1913
no. observed [$I \geq 2\sigma(I)$]	1617	1336
no. params	117	116
R1/wR2 [$I \geq 2\sigma(I)$]	0.0395, 0.1263	0.0414, 0.1182
R1/wR2 (all data)	0.0458, 0.1322	0.0605, 0.1297
GOF	1.075	1.001
$\Delta\rho$[c] e/Å^3	−0.525, 0.573	−0.289, 1.166

[a] Diffraction data were collected after virgin **1** was heated to 360 K at a rate of 2 K/min and cooled down to 298 K at a rate of −10 K/min. Then, intensity data for the amorphous phase were collected, followed by the exposure of the crystal to air for 1.5 h and data collection for the rehydrated phase. [b] This space group has the same symmetry as *Pnma* (No. 62), which is employed for uniform definition of the axes for comparison to ***2S*** (see Supporting Information).[11] [c] Minimum and maximum residual electron densities.

resulting in a higher symmetry space group, and X-ray analysis revealed that the two nitrogen atoms of ethylenediamine have fully occupied positions and are common to the equally disordered pair of carbon atoms. This also results in the two nearest cyanide groups of the Cr atoms of adjacent layers being equidistant from the coordinating oxygen atom of the water molecule (Figure 5). Therefore, we propose that, upon dehydration, there is equal probability for either cyanide to occupy the position of the leaving water molecule, unlike the case for ***2rac*** and **3**, and consequently causes severe disorder and a loss of crystallinity in the dehydrated crystal. On the other hand, rehydration repairs the faults and brings about a recovery of order within the structure. This hypothesis means that the layer is not altered and the loss of crystallinity is only due to stacking faults from layer to layer. This point is also suggested by the XRPD experiments (see below).

For ***2rac*** and **3**, the problem is not present, and therefore, the dehydration of a single crystal resulted in a well-ordered crystalline state. In the case of **3**, this can be described from the asymmetric nature between two cyanide groups in axial positions of the Cr ion. One side of the nitrogen atom on the cyanide group has a hydrogen bond with the water molecule coordinating to Mn in the adjacent layer, but the other side has a hydrogen bond with crystal water. However, the reversibility has unfortunately not been demonstrated. Also, severe disorder of the amine in **3** resulted in a high reliability factor R1 in both the virgin and dehydrated structure refinements.

Table 3. Selected Bond Distances, Angles, and Metal Separations for Virgin **1** and Rehydrated **1-HP**

	virgin **1**	rehydrated **1-HP**
Selected Bond Distances (Å) for Octahedral Geometries for Mn and Cr		
Mn(1)−N(1)	2.198(2)	2.199(2)
Mn(1)−N(2)	2.212(2)	2.210(2)
Mn(1)−N(4)	2.303(3)	2.299(4)
Mn(1)−O(1)	2.227(2)	2.231(3)
Cr(1)−C(1)	2.063(2)	2.069(3)
Cr(1)−C(2)	2.066(2)	2.074(3)
Cr(1)−C(3)	2.062(3)	2.062(3)
Selected Bond Angles (deg) for Octahedral Geometries for Mn and Cr[a]		
N(1)−Mn(1)−N(1)$^{\#1}$	90.06(13)	90.25(14)
N(1)−Mn(1)−N(2)	90.68(10)	90.63(11)
N(1)−Mn(1)−N(4)	92.75(8)	92.75(10)
N(1)−Mn(1)−O(1)	85.04(7)	85.03(9)
N(2)−Mn(1)−N(2)$^{\#1}$	88.56(12)	88.47(13)
N(2)−Mn(1)−N(4)	88.23(8)	88.18(10)
N(2)−Mn(1)−O(1)	94.01(8)	94.08(9)
N(1)−Mn(1)−N(2)$^{\#1}$	178.74(8)	178.68(10)
N(4)−Mn(1)−O(1)	176.87(11)	176.84(12)
C(1)−Cr(1)−C(2)	88.59(10)	88.76(12)
C(1)−Cr(1)−C(3)	89.14(10)	89.05(11)
C(1)−Cr(1)−C(2)$^{\#2}$	91.41(10)	91.24(12)
C(1)−Cr(1)−C(3)$^{\#2}$	90.86(10)	90.95(11)
C(2)−Cr(1)−C(3)	88.36(10)	88.22(11)
C(2)−Cr(1)−C(3)$^{\#2}$	91.64(10)	91.78(11)
Selected Bond Angles (deg) for Two-Dimensional Sheet[b]		
C(1)−N(1)−Mn(1)	170.9(2)	170.3(3)
C(2)$^{\#1}$−N(2)−Mn(1)	156.0(2)	156.2(2)
N(1)−C(1)−Cr(1)	177.1(2)	177.2(3)
N(2)$^{\#2}$−C(2)−Cr(1)	175.7(2)	175.7(3)
Distances for Hydrogen Bonds (Å)[c]		
N(5)···O(1)$^{\#1}$	2.937(4)	2.957(5)
N(5)···O(2)	2.831(9)	2.862(10)
O(1)···N(3)$^{\#2}$	2.752(4)	2.754(5)
O(1)···N(3)$^{\#3}$	2.752(4)	2.754(5)
Selected Intranetwork Metal Separations (Å) through One Cyanide Group[d]		
Mn(1)···Cr(1)^{A}	5.3802(5)	5.3890(6)
Mn(1)···Cr(1)$^{\#1,B}$	5.2813(5)	5.2920(6)
Mn(1)···Cr(1) (Ave.)	5.3308	5.3405
Selected Internetwork Metal Separations (Å)[e]		
Mn(1)···Cr(1)$^{\#1}$	7.4984(7)	7.5109(9)
Cr(1)···Cr(1)$^{\#2}$	8.3686(7)	8.3812(9)
Mn(1)···Mn(1)$^{\#3}$	8.3066(9)	8.3203(12)
Mn(1)···Mn(1)$^{\#4}$	8.4326(9)	8.4439(12)

[a] Symmetry code #1: $x, y - 1/2$. #2: $-x, -y, -z$. [b] Symmetry code #1: $x + 1, y, z$. #2: $x - 1, y, z$. [c] Symmetry code #1: $-x + 1/2, y, z + 1/2$. #2: $-x + 1/2, -y + 1/2, z - 1/2$. #3: $-x + 1/2, -y, z - 1/2$. [d] Symmetry code #1: $x + 1, y, z$. Metal separation through (A) C(1)−N(1), (B) C(2)−N(2). [e] Symmetry code #1: $x + 1/2, -y, z - 1/2$. #2: $x + 1/2, -y, -z + 1/2$. #3: $-x + 3/2, y, z + 1/2$. #4: $x - 1, y, z$.

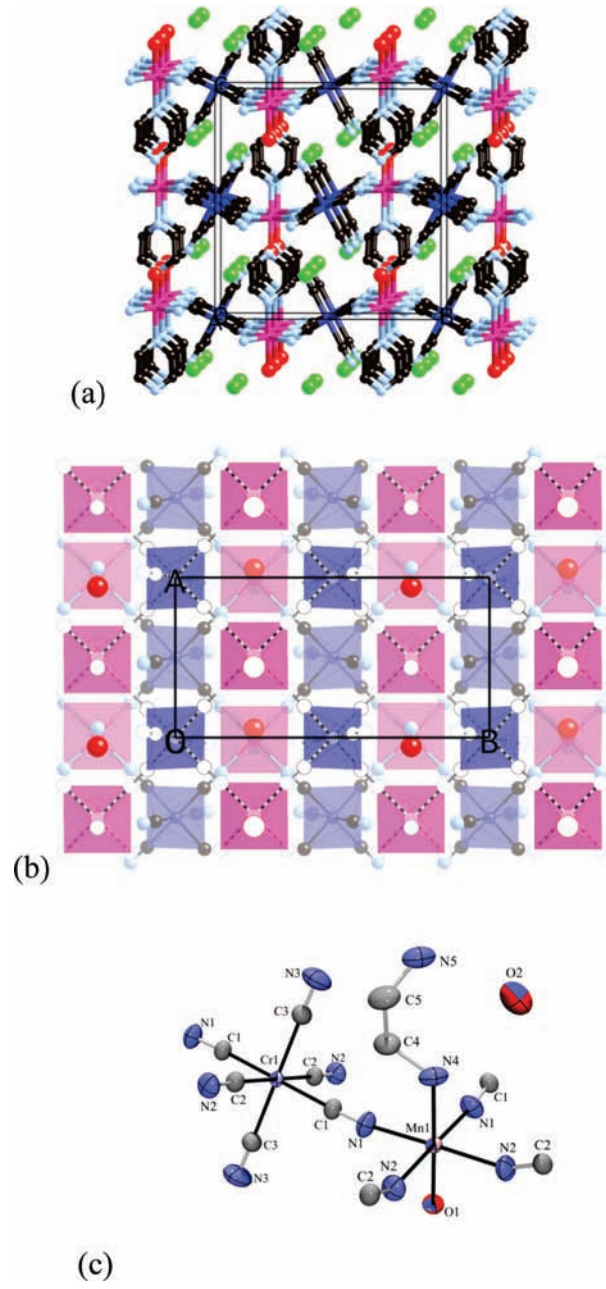

Figure 4. (a) Projection of the crystal structure along the *a* axis (left). Blue for Cr, pink for Mn, red for coordinating water, and green for noncoordinated water. (b) A view of two adjacent square-grid layers, one with broken bonds and open atoms and the other with solid bonds and filled atoms (right). The layer at the back is faded. (c) ORTEP drawing (bottom) for **1**.

Although there is clear evidence for incomplete reversibility in the TG measurements, the single-crystal X-ray analyses of **1-HP** do not reveal it. A plausible explanation is that the defects produced through dehydration−rehydration contribute to the background, which is not considered in the integration, and to broadening of the Bragg reflections, which results in larger errors for the refined parameters.

Powder X-Ray Diffraction. To verify that the structural changes taking place during dehydration and rehydration occur also for the bulk, powder X-ray diffraction spectra for each phase were collected by in situ measurement. Diffraction data for a virgin sample of **1** placed on a glass plate were collected using the Bragg−Brentano geometry. The same experiment for **1-DP** was performed after the sample of **1** had been dehydrated for 10 min at 360 K. Then, the data for the rehydrated sample of **1-HP** were collected after exposing the sample of **1-DP** to the air for 1 h. The results are shown in Figure 6 together with the diffraction pattern calculated from the single-crystal data. It is clear that the pattern for virgin **1** and that for rehydrated **1-HP** show almost the same pattern, indicating that dehydration is reversible. However, broadening of the lines, suggesting the loss of crystallinity, was always observed for the dehydrated samples.

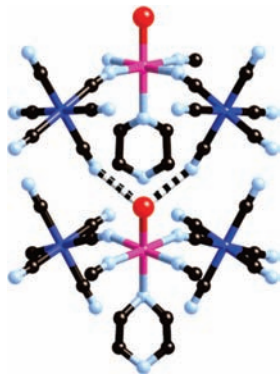

Figure 5. View of the two equally distant cyanide groups of one layer possible for coordination (striped bonds) upon departure of the water molecule (red) on the adjacent layer.

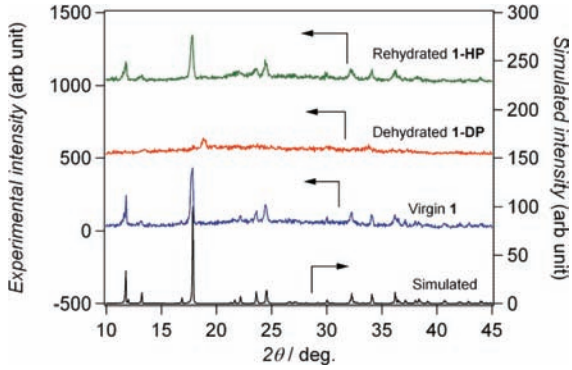

Figure 6. Experimental and simulated XRPD (Cu Kα) patterns for virgin **1**, dehydrated **1-DP**, and rehydrated **1-HP**.

Magnetic Properties. The temperature dependencies of the $\chi_M T$ values for **1**, **1-DP**, and rehydrated **1-HP** measured upon cooling in a field of 100 Oe are displayed in Figure 7a. The $\chi_M T$ values are 4.96, 4.90, and 4.90 cm^3 K mol^{-1} at 300 K, and they decrease upon lowering the temperature of the samples down to minima of 3.67 (90 K), 3.99 (120 K), and 3.70 (90 K) cm^3 K mol^{-1}, respectively. Upon further cooling, the $\chi_M T$ values increase to maxima of 951 (32 K), 2005 (55 K), and 1104 cm^3 K mol^{-1} (32 K) before decreasing below these temperatures, respectively. This temperature dependence of $\chi_M T$ is typical of ferrimagnets. The high-temperature region of χ_M for each phase follows the Curie−Weiss law ($\chi_M = C/(T - \theta)$) with a Weiss constant θ of −72.5, −83.7, and −73.2 K and Curie constant C of 6.20, 6.28, and 6.09 cm^3 K mol^{-1}, respectively (Figure 7b). These Curie constants are comparable to the theoretical value of 6.25 cm^3 K mol^{-1} expected for the sum of one Mn^{II} and one Cr^{III}. The negative Weiss constants indicate considerable antiferromagnetic interaction between the Cr^{III} ion and the Mn^{II} ions through the cyanide bridges.

In the ZFC and FC measurements in an applied field of 5 Oe, spontaneous magnetizations confirming long-range magnetic orderings are observed below 42, 75, and 42 (+65) K for **1**, **1-DP**, and rehydrated **1-HP**, respectively (Figure 7c; Table 4). These Curie temperatures were further confirmed by the observation of bifurcation in the ZFC−FC measurements for a different sample.

Given that the order of the average metal separations between Mn and Cr atoms within a layer is 5.3308(7) Å for

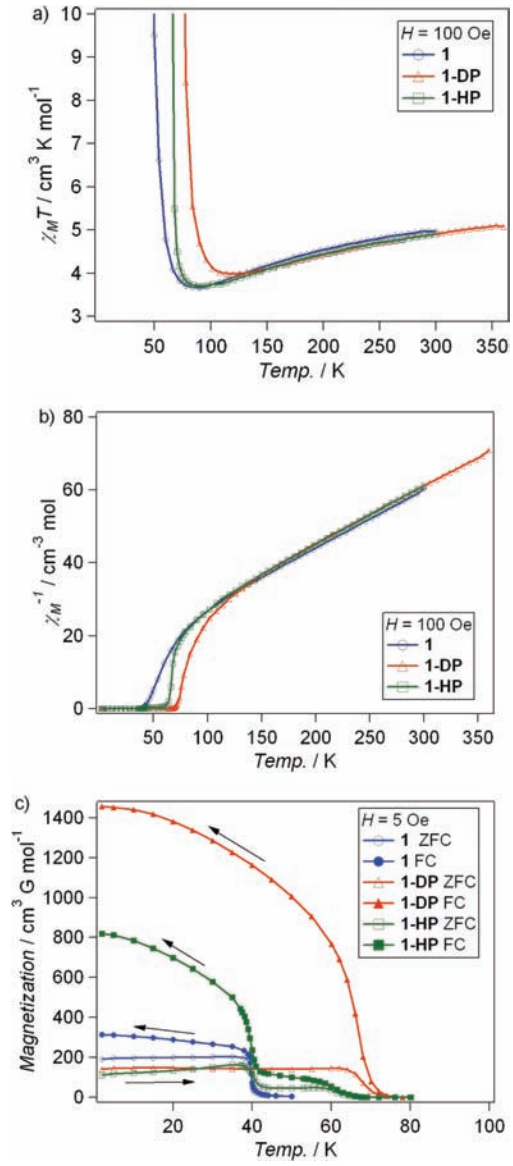

Figure 7. Temperature dependence of (a) $\chi_M T$, (b) χ_M^{-1}, and (c) zero-field-cooled and field-cooled magnetization for virgin **1**, dehydrated **1-DP**, and rehydrated **1-HP**.

Table 4. Magnetic Parameters for Virgin **1**, Dehydrated **1-DP**, and Rehydrated **1-HP**

	1	**1-DP**	**1-HP**[a]
fitting region/K	300−120	360−160	300−120
R^2 value	0.9998	0.9998	0.9998
C[b]/cm^3 mol^{-1} K	6.20	6.28	6.09
θ[c]/K	−72.5	−83.7	−73.2
T_{min}[d]/K	90	120	90
$\chi_M T$ (T_{min})/cm^3 mol^{-1} K	3.67	3.99	3.70
$\chi_M T$ (300 K)/cm^3 mol^{-1} K	4.96	4.90	4.90
T_C[e]/K	42	75	42 (+65)
M_{2K}[f]/cm^3 G mol^{-1}	480	1597	814
M_{sat}[g]/μ_B	2.02	2.05	2.04
H_C[h]/Oe	60	100	60
M_{REM}[i]/μ_B	0.36	0.67	0.51

[a] After soaked in distilled water. [b] Curie constants. [c] Weiss constants. [d] Temperatures at minimum values of $\chi_M T$. [e] Critical temperatures based on FC measurements. [f] Magnetization at 2 K in FC measurement (H = 5 Oe). [g] Magnetization saturation value at 2 K. [h] Coercive field at 2 K. [i] Remanent magnetization at 2 K.

1, 5.3490(14) Å for **2*S***,[21] and 5.3729(11) Å for **2*rac***,[6b] the small difference of T_C for **1** (42 K), **2*S*** (38 K), and **2*rac*** (36

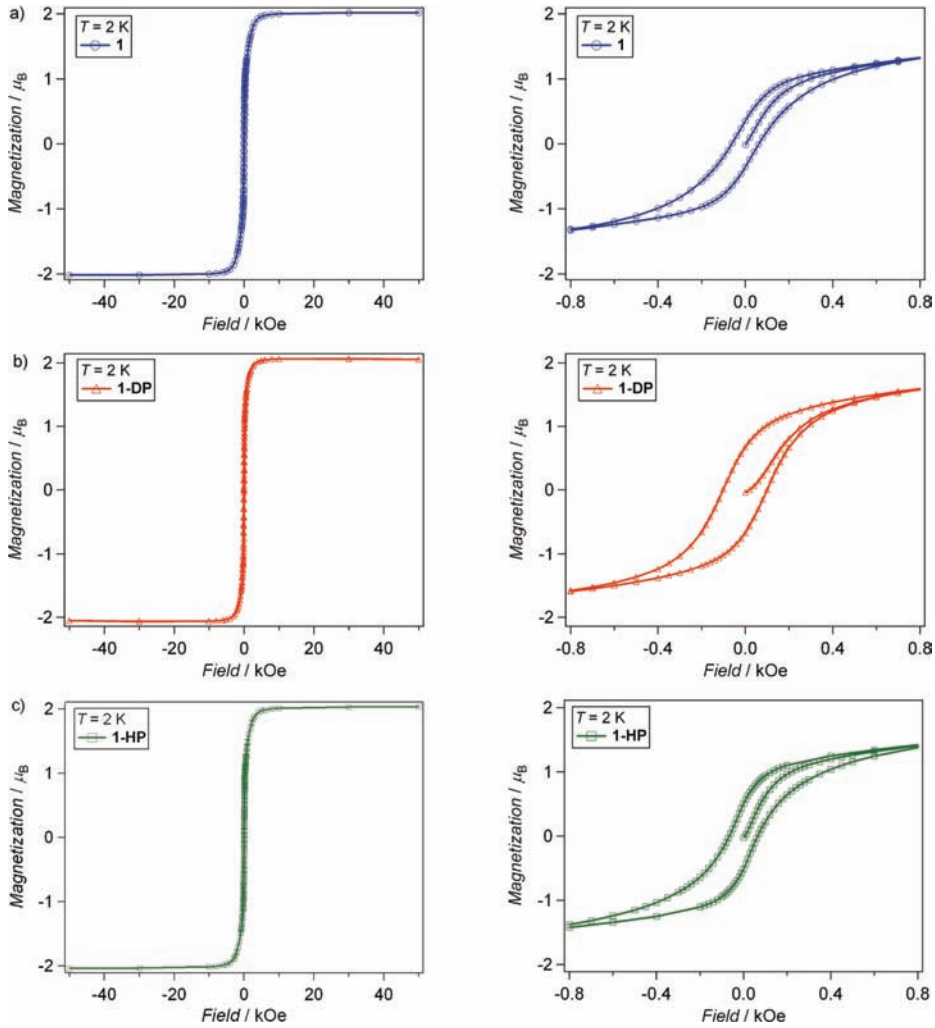

Figure 8. Field dependence of the magnetization at 2 K for (a) virgin **1**, (b) dehydrated **1-DP**, and (c) rehydrated **1-HP**.

K) can be a consequence of a slightly larger exchange coupling between Mn and Cr atoms through the cyanide group. However, the Curie temperature of **3** (35.2 K) is expected to lie between those of **1** and **2*S*** due to the average metal separations between Mn and Cr atoms for **3** (5.342(4) Å) being between those for **1** and **2*S***. It is worth noting that the nearest-neighbor and next-nearest-neighbor intersheet metal separations are found between heterometals (Mn···Cr, 7.378(3) Å) and homometals (Cr···Cr, 8.113(3) Å) for **3**, and these describe ferromagnetic and antiferromagnetic interaction, respectively. But these distances are found only between heterometals for **1** (7.4984(7) Å x2), **2*S*** (7.3239(7) and 7.7845(7) Å), and **2*rac*** (7.5376(11) × 2). These distances for **3** indicate weaker intersheet ferromagnetic interactions, which might be responsible for the lower Curie temperature.

For the dehydrated **2*rac*** and **3**, it has been shown by crystallography on single crystals that the structures transform into 3D networks through additional cyanide bridges between Cr and Mn from adjacent layers upon dehydration. This increase in dimensionality may also take place for **1-DP**, and consequently, T_C is significantly higher than for the virgin sample.

Upon rehydration of the previously dehydrated sample by soaking in water, the magnetization in a field of 5 Oe shows two anomalies: one at the Curie temperature of the virgin sample and the other at 65 K. While the one at 42 K indicates that the process of rehydration reverses the sample to the virgin state, the small magnetization trailing at higher temperatures indicates that some fragments of the sample retain the dehydrated form. These observations are in agreement with the TGA data, which suggest that only 93% transformation takes place after the first dehydration−rehydration cycle. However, the quantitative comparison is not possible due to the different rate of rehydration from sample to sample under the conditions at which the SQUID measurements were performed.

For every state of the compound, an almost square-shaped hysteresis loop was observed at 2 K (Figure 8). The observed saturation magnetization values for **1**, **1-DP**, and **1-HP** were 2.02, 2.05, and 2.04 μ_B, respectively, which are in good agreement with the theoretical value expected for ferrimagnets where antiferromagnetic coupling between Cr^{3+} and Mn^{2+} ions exists ($5/2g_{Mn} - 3/2g_{Cr} = 2$, if $g = 2$). The observed remanent magnetization and coercive field of the hysteresis loops are 0.36, 0.67, and 0.51 μ_B and 60, 100,

and 60 Oe, respectively. These values suggest that **1** is a soft ferrimagnet, while it slightly hardens upon dehydration and recovers the initial softness by rehydration. A similar effect was observed for **3**.[5] The initial magnetization against the field for **1** and **1-HP** appears to be of the nucleation type, while that of **1-DP** is of the pinning type.[22] This suggests that the magnetic domains are more anisotropic for **1-DP** than for **1** and **1-HP**, and therefore, the moments are more easily reversed for **1** and **1-HP**.

Conclusion

In summary, $[Mn^{II}(enH)(H_2O)][Cr^{III}(CN)_6]\cdot H_2O$ displays a two-dimensional square grid of alternating Mn and Cr connected by cyanide, which behaves as a ferrimagnet below a Curie temperature of 42 K. It is inferred that it retains its layer arrangements during dehydration but loses coherence due to statistical disorder in forming a three-dimensional framework, which behaves also as a ferrimagnet at an elevated Curie temperature of 75 K. Upon rehydration, the coherence is recovered, and the crystal structure was determined. However, thermogravimetry cycling suggests only partial recovery, which decreases with the number of cycles.

Acknowledgment. This work was supported by a Grant-in-Aid for Science Research (A) (No. 18205023) from the Ministry of Education, Science, Sports, and Culture and the CNRS (France). Y.Y. thanks the Université Louis Pasteur for its hospitality during his stay in Strasbourg.

Supporting Information Available: A synthesis description and additional figures and tables (PDF) and crytsal data (CIF). This material is available free of charge via the Internet at http://pubs.acs.org.

IC801734X

(22) Bertotti, G. *Hysteresis in magnetism: for physicists, material scientists, and engineers*; Academic Press: San Diego, 1998; p 318.